American Journal of Medical Genetics 107:317–324 (2002)

# Craniofacial Phenotypes in Segmentally Trisomic Mouse Models for Down Syndrome

**Joan T. Richtsmeier,[1,2]* Ann Zumwalt,[3] Elaine J. Carlson,[4] Charles J. Epstein,[4] and Roger H. Reeves[5]**

[1]*Department of Anthropology, Pennsylvania State University, University Park, Pennsylvania*
[2]*Center for Craniofacial Development and Disorders, Johns Hopkins Hospital, Baltimore, Maryland*
[3]*Department of Cell Biology and Anatomy, Johns Hopkins University School of Medicine, Baltimore, Maryland*
[4]*Department of Pediatrics, University of California, San Francisco, California,*
[5]*Department of Physiology, Johns Hopkins University School of Medicine, Baltimore, Maryland*

**Trisomy for chromosome 21 (Chr 21) has profound effects on development that result in a constellation of phenotypes known as Down syndrome (DS). Distinctive craniofacial manifestations are among the few features common to all individuals with DS. The characteristic face of a person with DS results primarily from maldevelopment of the underlying craniofacial skeleton. The Ts65Dn mouse, which has segmental trisomy 16, producing dosage imbalance for about half the genes found on human Chr 21, exhibits specific skeletal malformations corresponding directly to the craniofacial dysmorphogenesis in DS. Here we demonstrate that Ts1Cje mice, which are at dosage imbalance for about 3/4 of the genes triplicated in Ts65Dn, demonstrate a very similar pattern of anomalies in the craniofacial skeleton. However, one characteristic of Ts65Dn mice, a broadening of the cranial vault contributing to brachycephaly, is not seen in Ts1Cje mice. These observations independently confirm that a dosage imbalance for mouse genes orthologous to those on human Chr 21 has corresponding effects in both species. The subtle differences in the craniofacial phenotypes of Ts1Cje and Ts65Dn mice have implications for elucidation of the mechanisms by which this aneuploidy disrupts development.**


**KEY WORDS: Down syndrome; trisomy; aneuploidy; Ts1Cje; Ts65Dn; mouse models; skull; morphometrics**

## INTRODUCTION

Trisomy 21 (Ts21) produces the clinical entity known as Down syndrome (DS) (MIM 190685) [LeJeune et al., 1959]. DS is characterized by a number of features that distinguish individuals with three rather than two copies of chromosome 21 (Chr 21). Although the overall pattern of abnormalities is quite characteristic, only a subset of the features are present in any individual with Ts21, and only a few features are present in all individuals with DS [Epstein, 1986]. Among these, the distinctive craniofacial appearance is a constant and immediately recognizable phenotype of DS. Several quantitative studies (primarily using roentgencephalometric methods) have shown that these features reflect, in part, developmental anomalies of the craniofacial skeleton. Features that have been defined qualitatively and quantitatively in humans with DS include overall reduction in skull size, determined by a generalized reduction in all measures taken on a lateral cephalogram; a flattened occiput, noted on observation and reflected in a reduction in cranial length; brachycephaly, measured as an increase in the cranial breadth/length ratio; a small midface, reflected in measures that traverse the nasomaxillary complex; a reduced maxilla, reflected in measures of the palate and alveolar segments; reduced interorbital distance; and a reduced mandible, as measured on the ramus [Kisling, 1966; Fink et al., 1975; Farkas et al., 1985] (Fig. 1). Although craniofacial effects are an invariant aspect of DS, a great amount of individual metric variation in these craniofacial features and in other metric phenotypes has been reported among DS individuals [Kisling, 1966; Thelander and Pryor, 1966; Frostad et al., 1971; Cronk and Reed, 1981].

Two mouse strains with segmental trisomy 16 have been studied as genetic models of DS. Ts65Dn mice,

Grant sponsor: Public Health Service; Grant numbers: 1F33DE/HD05706, HD 31498, HD38384, HD24605.

*Correspondence to: Joan T. Richtsmeier, Department of Anthropology, 320 Carpenter Bldg., Pennsylvania State University, University Park, PA 16802. E-mail: jta10@psu.edu

Received 21 May 2001; Accepted 5 October 2001


DOI 10.1002/ajmg.10175

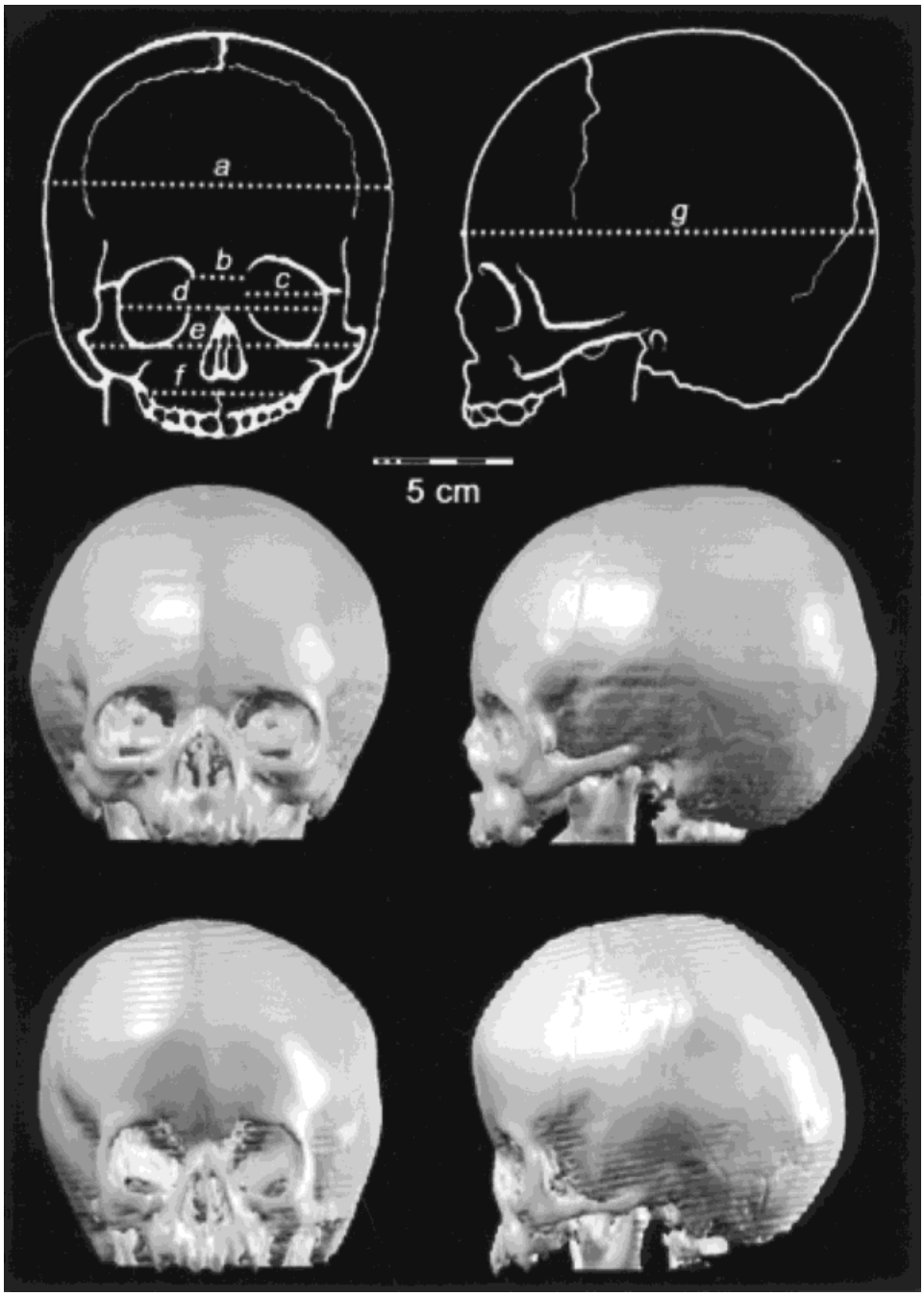


Fig. 1. 3D reconstructions of computed tomography scans of a Down syndrome male individual at 1 year 8 months (bottom row) and an unaffected individual matched for age and sex (middle row). These images were chosen as examples from our archives and are not meant to represent an average skull of a DS individual or the average normal human configuration for this age. Some of the quantitative differences in the DS cranium that have been demonstrated previously are shown on the line drawing (top row). These include brachycephaly, a neurocranium that is wide relative to a measure of skull length (**a**); a reduced interorbital distance (**b**); a reduced width of the orbit (**c**); a reduced bi-orbital breadth (**d**); a reduced bi-zygomatic breadth (**e**); and a reduced maxillary width (**f**). A general reduction in facial dimensions is also apparent in the DS individual.

produced by Davisson and colleagues [Davisson et al., 1990], have segmental trisomy 16 for a region that corresponds to a segment of human chromosome 21 (HSA 21) that spans 15.6 Mb and contains the orthologs of 108 of the 225 expressed sequences identified in the HSA 21 gene catalog [Hattori et al., 2000]. A second segmental trisomy 16 mouse model, Ts1Cje, arose as a fortuitous translocation of mouse chromosome 16 (MMU 16) in a mouse line produced by homologous recombination at the *Sod1* locus [Sago et al., 1998]. Ts1Cje mice are at dosage imbalance for a subset of genes triplicated in Ts65Dn. This smaller segment

corresponds to a region of HSA 21 that spans 9.8 Mb and contains 79 genes, or 73% of the number triplicated in Ts65Dn mice.

We recently reported the results of a detailed analysis of the skull of adult Ts65Dn mice and their normal littermates that demonstrated direct parallels between the dysmorphology associated with the human DS craniofacial phenotype and that of the Ts65Dn skull [Richtsmeier et al., 2000]. These results were obtained through precise measurement of three-dimensional coordinates of biological landmarks on the skull and analysis by a co-ordinate system invariant morphometric technique, Euclidean Distance Matrix Analysis (EDMA) [Lele and Richtsmeier, 2001]. When compared statistically to the skulls of normal littermates, the Ts65Dn craniofacial skeleton showed an overall reduction in size; a disproportionately reduced midface, maxilla, and mandible; reduced interorbital breadth; and a reduced occipital region. The current study examines the Ts1Cje skull. We demonstrate that the Ts1Cje skull shows the same direct parallels to the DS craniofacial phenotype. Skulls of Ts1Cje and Ts65Dn aneuploid mice differ from their respective euploid littermates in similar ways, even though the number of genes at dosage imbalance is not the same in the two mouse models.

## MATERIALS AND METHODS

Production of B6C3HF1-Ts65Dn and littermate control mice was described previously [Richtsmeier et al., 2000]. Ts65Dn mice are maintained by continually intercrossing female Ts65Dn mice to male (C3H $\times$ B6) F1 mice. To duplicate the genetic background of this population, Ts1Cje mice that were inbred onto the C57BL/6 background were crossed with C3H/HeJ mice. The F1 animals were crossed to (B6 $\times$ C3H) F1 mice. Trisomic mice were identified by PCR as described by Sago et al. [1998]. Litters of adult mice 14 weeks of age were euthanized. An additional litter containing three euploid and two aneuploid mice were euthanized at 10 weeks. All litters were included in analysis. The results presented here are consistent with results of analyses that do not include the single 10-week-old litter. Heads were skinned and stripped of excess neural and muscular structures and put into a Dermestid beetle colony for cleaning.

Three-dimensional coordinate locations of 49 landmarks located on the cranium and mandible of Ts1Cje mice ($N = 12$) and normal littermates ($N = 15$) were collected using the Reflex microscope [Richtsmeier et al., 2000]. The observer was blinded to the karyotype of each mouse during data collection. Landmark coordinate data were analyzed for DS using EDMA to provide a statistical test of similarity in craniofacial form between mouse models and their normal littermates. A null hypothesis of similarity in shape for portions of the craniofacial skeleton defined by a specific subset of landmarks is tested using a nonparametric bootstrapping procedure [Lele and Richtsmeier, 1991]. $P$ values report the significance level for testing the null hypothesis. Landmark subsets are formed based on prior biological knowledge and are used because the total number of landmarks is greater than the sample size, precluding statistical testing of the entire craniofacial complex. Specifically, subsets are designed to capture the shape of specific aspects of the adult human skull (e.g., midface, consisting primarily of the maxilla and zygoma; orbital region; and posterior cranial vault) or developmental units, or to designate corresponding features in the mouse skull already demonstrated as affected in the DS skull. Because variability is critical to understanding the biological basis for differences in morphology, we also use nonparametric bootstrapping to calculate confidence intervals ($\alpha = 0.10$) for all linear distances being compared between segmentally trisomic mice and euploid littermates [Lele and Richtsmeier, 1995]. These confidence intervals enable localization of similarities and differences in form.

Additional methods permit statistical comparison of the within-model comparisons. Results of the Ts65Dn-to-euploid analysis are compared to the Ts1Cje-to-euploid analysis for each subset of landmarks by null hypothesis testing [Richtsmeier and Lele, 1993] and for all linear distances among landmark pairs using confidence intervals [Lele and Richtsmeier, 1995]. The null hypothesis for these comparisons is that the difference in shape between the Ts65Dn mice and their normal littermates is similar to the difference in shape between the Ts1Cje mice and their normal littermates. Confidence intervals determine if the difference measured between Ts65Dn mice and normal littermates at each linear distance is the same as that measured between Ts1Cje mice and their normal littermates.

## RESULTS

### Cranium

The crania of Ts1Cje mice differ from normal littermates in ways that parallel the differences seen between the crania of humans with Ts21 and unaffected individuals (Fig. 2). The entire Ts1Cje cranium is reduced along the anteroposterior (AP) axis, and the face is disproportionately affected, compared to the neurocranium. Facial dimensions are reduced by 6% on average, compared to a 4% average reduction in the cranial vault. The reduction of the cranial vault along the AP axis is greater on average (by 2%) than along the mediolateral axis. Thus, the Ts1Cje cranium is brachycephalic (short relative to its width), compared to normal littermates. Brachycephaly is characteristic of the DS cranium [e.g., see Kisling, 1966]. Finally, the interorbital breadth is reduced in Ts1Cje mice. Reduction of interorbital distance is a characteristic of DS and was also found in the Ts65Dn mouse model.

Sixteen biologically relevant landmark subsets (Table I; Fig. 2) were designed to represent developmental and structural units of the cranium [Richtsmeier et al., 2000]. Using these subsets, we tested the null hypothesis of similarity in shape between aneuploid and euploid littermates and found that both Ts1Cje and Ts65Dn differed significantly from controls ($P \leq 0.05$). We then tested the null hypothesis of comparable differences in shape between the Ts65Dn-to-euploid

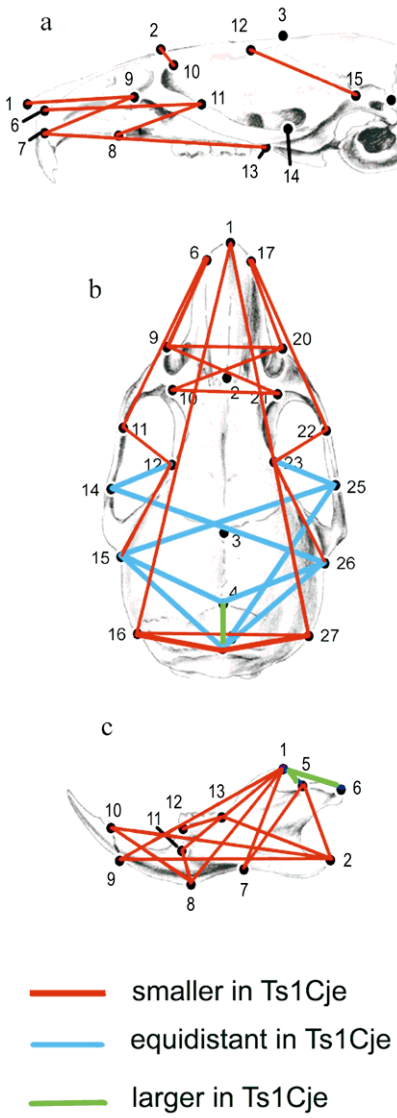


Fig. 2. Normal mouse cranium and mandible with locations of landmarks used in analysis and differences between euploid and aneuploid Ts1Cje mice indicated: lateral view of cranium (**a**), superior view of cranium (**b**), and lateral view of mandible (**c**). Lines show a subset of those linear distances that are significantly different between Ts1Cje aneuploid and euploid littermates by confidence interval testing (in red and green), as well as some linear distances that are not affected by aneuploidy (in blue). Of the 351 linear distances, 79% are significantly different between euploid and aneuploid littermates.

comparison and the Ts1Cje-to-euploid comparison. We could not reject the null hypothesis of similarity in relative dysmorphology for Ts1Cje and Ts65Dn (for all subsets, $P > 0.21$; Table I, column 3), indicating that both mouse models differ from their respective euploid littermates according to similar anatomical patterns. These results demonstrate a high degree of correspondence in the patterns of shape difference that distinguish each segmentally trisomic model from its normal littermates.

Confidence intervals were estimated to compare individual linear distances and provide information concerning variation within a sample. Of the 351 unique linear distances that can be constructed from the 27 cranial landmarks, 81% (286 linear distances) are affected similarly in the two segmentally trisomic mouse models. Of these 286 linear distances, 217 are significantly different from euploid littermates in both mouse models, while 69 distances are similar within each trisomy:euploid set. These 69 measurements represent particular dimensions of the craniofacial skeleton that are not affected by segmental trisomy in either model. The remaining 65 linear distances (19% of the total) are affected differently in Ts65Dn and Ts1Cje mice.

The 65 linear distances that are affected differently in the two models are shown in Figure 3. The linear distances that are reduced in Ts1Cje but not in Ts65Dn (Fig. 3a) cross the maxillae and frontal and parietal bones along all three axes, but most frequently along the AP and superoinferior axes. Those measures that are reduced in Ts65Dn but not affected in Ts1Cje (Fig. 3b) cross the maxillae, frontal and parietal bones, and occipital bones along the AP and mediolateral axes. Though the concentration of these measures appears relatively more anterior on inspection, a few linear distances stretch back to the occiput (see Fig. 3b, landmarks 5 and 27), suggesting a more generalized shortening of the Ts65Dn skull along the AP axis.

Seven distances spanning the mediolateral axis of the posterior neurocranium and two more that describe the height of the neurocranium measured from the posterior palate (landmarks 13 and 24) to bregma are uniquely affected in Ts65Dn and have no corresponding trend in Ts1Cje (Fig. 3b). These characters describe an expanded Ts65Dn aneuploid neurocranium local to the parietal bones along mediolateral and superoinferior axes.

## Mandible

Atchley and Hall [1991] provided a model for development and evolution of the mammalian mandible that is useful in our comparison of Ts65Dn and Ts1Cje. The mandible is composed of right and left sides, each consisting of a single dentary bone. Each dentary bone develops from six semi-independent morphogenetic units: the horizontal ramus; the molar and incisor alveolar components; and the coronoid, condylar, and angular processes (Fig. 4a). To propose a developmental basis for the differential effects of segmental trisomy in the two mouse models, we devised five subsets of landmarks for analysis based on functional combinations of these six morphogenetic units (Table II).

Ts1Cje mandibles differ significantly from their respective euploid littermates (Fig. 2c) according to a pattern similar to that reported previously for Ts65Dn [Richtsmeier et al., 2000]. The mandible is significantly smaller in all dimensions in both Ts1Cje and Ts65Dn, a finding that parallels a reduction in the mandibular ramus of individuals with DS [Kisling, 1966]. The linear distances that are larger in the Ts1Cje aneuploid

TABLE I. Results of Null Hypothesis Testing for the Cranium Landmark Subsets

| Subset name | Landmarks included in subset | *P*-values, TS1Cje-to-euploid comparison | *P*-values Ts65Dn-to-euploid comparison | *P*-values, Ts1Cje-to-euploid compared to Ts65Dn-to-euploid |
|---|---|---|---|---|
| Neuro 2 | 3 4 5 10 12 15 16 21 23 26 27 | 0.008 | 0.006 | 0.735 |
| One side | 1 3 4 5 7 8 9 10 11 12 13 14 15 16 | 0.002 | 0.002 | 0.509 |
| Maxilla l | 8 9 10 11 13 19 20 21 22 24 | 0.066 | 0.154 | 0.842 |
| Maxilla 2 | 8 9 10 11 13 | 0.002 | 0.002 | 0.901 |
| Maxilla 3 | 19 20 21 22 24 | 0.072 | 0.024 | 0.693 |
| Vault 1 | 2 3 4 5 12 16 23 27 | 0.092 | 0.004 | 0.723 |
| Vault 2 | 3 4 5 15 16 26 27 | 0.040 | 0.006 | 0.914 |
| Midface 1 | 6 10 13 17 21 24 | 0.104 | 0.244 | 0.601 |
| Midface 2 | 1 3 6 8 13 17 19 24 | 0.283 | 0.307 | 0.998 |
| Midface 3 | 1 3 6 8 9 13 17 19 20 24 | 0.299 | 0.325 | 0.998 |
| Neuro 1 | 3 4 12 15 23 26 | 0.098 | 0.204 | 0.814 |
| Orbit 1 | 9 10 11 14 20 21 25 | 0.002 | 0.010 | 0.321 |
| Orbit 2 | 11 14 22 25 | 0.006 | 0.024 | 0.210 |
| Orbit 3 | 9 10 11 14 20 21 22 25 | 0.004 | 0.020 | 0.473 |
| Orbit 4 | 2 3 9 10 11 12 20 21 22 23 | 0.042 | 0.062 | 0.567 |
| Symmetry | 8 9 10 13 19 20 21 24 | 0.212 | 0.311 | 0.984 |

Results of statistical tests of the null hypothesis of similarity in shape for the comparison of Ts1Cje-to-euploid (column 3) and Ts65Dn-to-euploid (column 4) and of the null hypothesis of similarity in shape differences of the comparisons of each DS mouse model to its normal littermates (column 5). Landmark subsets representing craniofacial anatomical components are used to ensure that the number of landmarks in each test is smaller than the number of individuals in the samples.

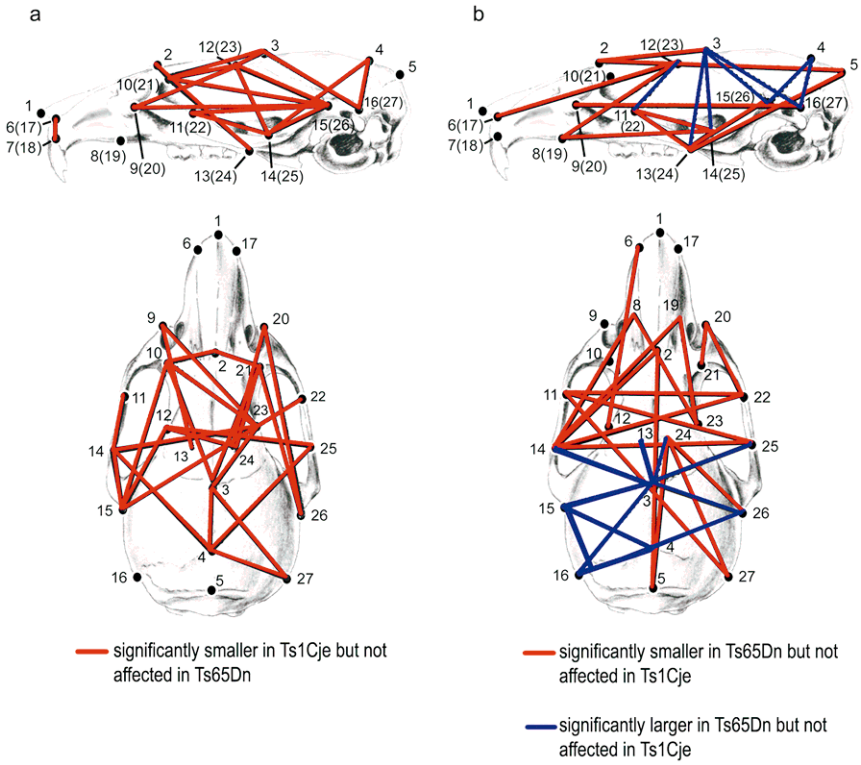


Fig. 3. Differential effects of aneuploidy in Ts1Cje (panel a, left) and Ts65Dn (panel b, right). In both panels a lateral view (top) and a superior view (bottom) of the normal mouse cranium are shown. **a:** Linear distances that are significantly reduced in Ts1Cje but not in Ts65Dn are shown in red and located in the central portion of the cranium, primarily along the AP and mediolateral axes. These linear distances cross the more superoposterior aspects of the face and the more anterior aspects of the neurocranium. **b:** Linear distances that are significantly different from euploid littermates in Ts65Dn but not in Ts1Cje have broad coverage. Reductions in palatal dimensions are included, as well as distances that connect palatal landmarks to those on the superior surface of the anterior face and neurocranium. Posterior aspects of the Ts65Dn neurocranium are expanded (purple lines), compared to euploid littermates, a pattern not seen in Ts1Cje. Some of these differences between Ts1Cje and Ts65Dn may reflect individual adjustments to a developmental program requiring reduction in overall craniofacial size.

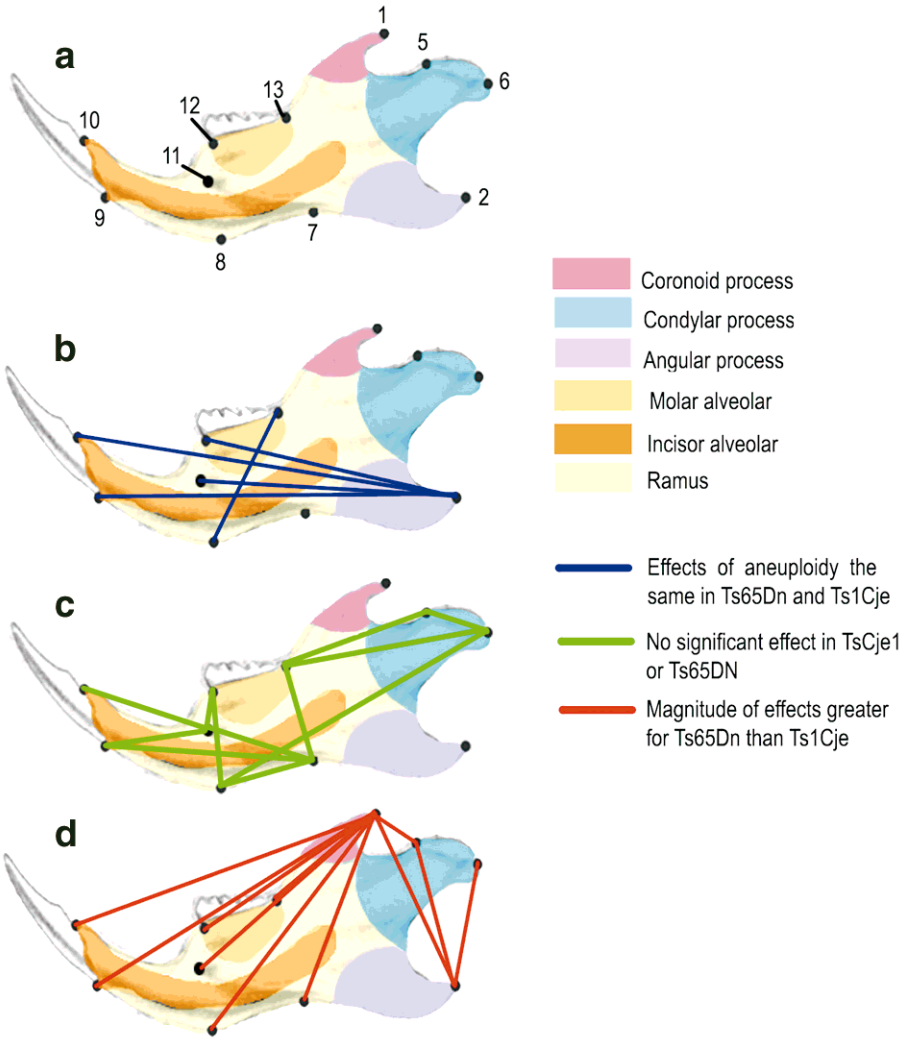


Fig. 4. **a:** Normal mouse hemimandible subdivided into the mandibular morphogenetic units proposed by Atchley and Hall [1991]. **b:** Superimposed on the mouse mandible are those linear distances in which the effects of aneuploidy are quantitatively similar in the two mouse models. **c:** There is no significant difference in aneuploid specimens, compared to euploid in Ts65Dn and Ts1Cje (in green). **d:** Those in which the effects are significantly greater in Ts65Dn (in red). Many of the other mandibular dimensions that are significantly reduced in Ts1Cje (Fig. 2) are more profoundly affected in Ts65Dn.

mice (Fig. 2c) indicate a reduction in the coronoid process, causing the distance between coronoid and condylar processes to increase. Both mouse models reveal a generalized effect on the entire mandible and a localized effect that is specific to the coronoid and angular processes.

Results of the null hypothesis test of similarity in shape between aneuploid and euploid mandibles for the two mouse models are given in Table II. Three of the five landmark subsets show the mandibles of Ts1Cje and Ts65Dn to be affected similarly. In the molar-and-incisive-alveolar subset and the ramus-and-alveolar

TABLE II. Results of Null Hypothesis Testing for the Mandible

| Subset name | Landmarks included in subset | *P*-values, TS1Cje-to-euploid comparison | *P*-values, Ts65Dn-to-euploid comparison |
|---|---|---|---|
| Angle, coronoid processes | 1 2 5 6 | 0.073 | 0.003 |
| Ramus | 7 8 11 | 0.007 | 0.037 |
| Molar and incisive alveolar | 7 8 12 13 | 0.043 | 0.512 |
| Ramus and alveolar | 7 8 9 10 11 12 13 | 0.017 | 0.243 |
| Ramus and processes | 1 2 5 6 7 8 11 | 0.017 | 0.003 |

*P*-values obtained from the test of the null hypothesis of similarity in shape for mandibular subsets. These mandibular landmark subsets are based on combinations of the 6 morphogenetic components proposed by Atchley and Hall [1991].

subset, the Ts1Cje mandible is significantly altered and the Ts65Dn mandible is not. Methods developed specifically for determining influential landmarks and confidence interval testing determine that a single linear distance is responsible for the different *P* values calculated for these subsets. The distance between the most anterior and most posterior points on the molar alveolar (landmarks 12 and 13, respectively) is significantly smaller than normal in Ts1Cje, but not in Ts65Dn. Differences in the Ts1Cje and Ts65Dn molar alveolar drive the statistically based morphological difference for this subset.

The different *P* values calculated for the ramus-and-alveolar-processes subset also reflect a localized difference in the effects of aneuploidy between Ts1Cje and Ts65Dn mice. The location of landmark 7 (Fig. 4a), at the intersection of the angular process with the corpus, is highly variable. Differences in variability at the base of the ramus are responsible for this result. Repeatability studies show that the variability is biologically based and not due to measurement error (data not shown).

Confidence intervals facilitate identification of distinctive patterns of local dysmorphology in the two mouse models. Confidence intervals confirm that the Ts1Cje mandible shows a significant reduction in the molar alveolar (landmarks 12 and 13, Fig. 2c), a feature not seen in Ts65. The Ts65Dn mandible shows a localized reduction in the height of the incisive alveolar segment, compared to a localized (but not significant) increase in this segment in Ts1Cje. Confidence intervals also demonstrate that the coronoid and angular processes are reduced in both Ts65Dn and Ts1Cje. Though the magnitude of the effects on the angular process and its relation to anterior points on the mandible are similar in the two models, its relation to the condylar and coronoid processes is more profoundly affected in Ts65Dn (see Fig. 4d). The coronoid process is more reduced in Ts65Dn, as shown in its position relative to the molar alveolar, the incisor alveolar, and points on the ramus.

## DISCUSSION

The mammalian cranium and mandible form a complex skeletal structure. The overall shape of the skull is dependent upon the coordinated development of separate bony, dental, and cartilaginous elements and functioning soft-tissue components. A cascade of developmental processes is necessary for the proper development of a functioning skull. The intricate harmony of the various genetically regulated developmental programs required during ontogeny can generate individual variability, thereby providing the raw material for the evolution of new phenotypes. We are beginning to understand the nature and ordering of these processes, including the role of major genes that function during each morphogenetic stage [Hall and Miyake, 1995; Hall, 1999; see Hall and Miyake, 2000].

Our analyses of the adult skulls of two segmentally trisomic mouse models for DS show that the morphology of the skull and dentary are affected by dosage imbalance and that specific craniofacial components are affected disproportionately. More than 80% of the euploid-to-aneuploid differences and similarities measured on the skull and dentary are conserved between the two mouse models for DS, even though the Ts65Dn mouse has many more genes at dosage imbalance. The faces of segmentally trisomic mice are especially reduced in size, and brachycephaly exists in both mouse models, though perhaps produced by different developmental perturbations, since the cranial vault is increased mediolaterally in Ts65Dn but not affected in Ts1Cje.

The entire mandible is smaller in both models, as it is in humans with DS. Since the length of the molar alveolar is significantly smaller than normal in Ts1Cje but unaffected in Ts65Dn, we examined the possibility of differential effects on developing teeth in the two models. The lengths of $M_1$ (first mandibular molar) and $M_2$ were recorded for all Ts65Dn and Ts1Cje mice directly from the lingual surface of left hemimandibles using the Reflex microscope. Confidence interval testing shows that the length of $M_1$ in aneuploid specimens of Ts1Cje and Ts65Dn is significantly smaller, relative to normal littermates. This suggests that tooth development is affected similarly in the two models and that the differences found in the effects of aneuploidy on the molar alveolar in the two models are due to differences in the development of bone. Support for this finding requires specific study of $M_1$, $M_2$, and $M_3$, including measures other than simple tooth lengths.

We localized areas that are not affected by aneuploidy in either model and observed similar effects in the two models local to the angular process (Fig. 4). Ts65Dn mice demonstrated appreciably amplified effects local to the coronoid process. The angular and coronoid processes develop in intimate contact with muscles of mastication. The angular process is associated with the medial pterygoid and the superficial massetor muscles while the coronoid process is associated with the temporadis muscle. Experiments with quail-chick chimeras have shown that a single population of neural crest cells is responsible for the formation of specific craniofacial muscles, as well as those portions of the bone to which the muscle attaches [Kontges and Lumsden, 1996]. The biomechanical influences of craniofacial muscles on the formation of the skull [Washburn, 1947; Horowitz and Shapiro, 1951; Moss and Meehan, 1970; Moore, 1973], as well as the dynamics of neural crest migration, are two potential sources of the effects on the angular and coronoid processes demonstrated in these two mouse models.

Comparison of magnitudes of the differences between Ts1Cje and normal littermates and Ts65Dn and their normal littermates indicates that the skulls of Ts65Dn mice are affected to a slightly greater degree, though this difference does not consistently reach statistical significance. In some locations, like the coronoid process of the mandible, there is a marked difference in the effects in the two models. The differential localized effects may be caused by gene action specific to these morphogenetic skeletal units or by gene action that affects the local environment, including but not limited to the influences of muscle size and action on

the developing bone, the interaction of developing tooth buds and surrounding skeletal components, and the influence of articulating skeletal units.

Overall, these results are notable for the similarity of the effects produced in Ts65Dn and Ts1Cje mice despite there being substantially more genes at a dosage imbalance in the former. This similarity from two independently generated models demonstrates that a dosage imbalance and not secondary effects of the translocations that generated the segmental trisomies is responsible for disrupting development in a specific manner. Moreover, the same bones of the skull are affected in a similar manner in DS, suggesting that the perturbation affects an evolutionarily conserved genetic pathway in an analogous fashion in these divergent mammalian species.

For all but a minority of characters that are significantly affected only in Ts1Cje, a similar trend is evident in Ts65Dn. Most of the significant changes in Ts65Dn mice show a similar trend in Ts1Cje mice as well. However, the significant broadening of the mediolateral dimensions of the cranial vault is unique to Ts65Dn mice. This difference may be explained by the presence in Ts65Dn mice of three copies of a specific gene or genes that are present in two copies in Ts1Cje mice and that act to produce this character when triplicated. Alternatively, the substantially larger genetic insult in Ts65Dn (approximately 108 genes triplicated vs. 79 in Ts1Cje) might destabilize a number of developmental pathways, thereby disrupting canalization of skull (and brain) development, while the less-disrupted Ts1Cje genome is better able to maintain homeostasis of this process. The former hypothesis can be tested by examining the skulls of Ms1CjeTs65Dn mice that are segmentally trisomic for only that segment not shared by Ts1Cje and Ts65Dn [Sago et al., 2000]. Alternatively, it can be tested by the construction of mice transgenic for each of the 28 genes present in this region to determine whether one of these genes causes a specific, quantitative broadening of the posterior cranium when present in three copies. The combination of molecular tools and morphometric techniques that enable precise measurement of the phenotype can bring us closer to understanding the production of morphology, thereby bridging the gap between genotype and phenotype.

## ACKNOWLEDGMENTS

We thank Linda Gordon of the National Museum of Natural History and Mark Mooney and Ronal Mitchell of the University of Pittsburgh for the use of their beetle colonies and technical expertise in cleaning of mouse skeletons. Valerie DeLeon prepared Figure 1. Erin Lindsay prepared Figure 4. This work was supported in part by Public Health Service awards 1F33DE/HD05706 (J.T.R.), HD 31498 (C.J.E.), and HD38384 and HD24605 (R.H.R. and J.T.R.).

## REFERENCES

Atchley W, Hall B. 1991. A model for development and evolution of complex morphological structures. Biol Rev 66:101–157.

Cronk C, Reed R. 1981. Canalization of growth in Down syndrome children three months to six years. Hum Biol 53:383–398.

Davisson MT, Schmidt C, Akeson E. 1990. Segmental trisomy of murine chromosome 16: a new model system for studying Down syndrome. Prog Clin Biol Res 360:263–280.

Epstein C. 1986. The consequences of chromosome imbalance: principals, mechanisms, and models. 16th ed. Cambridge: Cambridge University Press. 486 pp.

Farkas L, Munro I, Kolar J. 1985. Abnormal measurements and disproportions in the face of Down's syndrome patients: preliminary report of an anthropometric study. Plast Reconstr Surg 75:159–167.

Fink G, Madaus W, Walker G. 1975. A quantitative study of the face in Down's syndrome. Am J Orthod 67:540–553.

Frostad W, Cleall J, Melosky L. 1971. Craniofacial complex in the Trisomy 21 syndrome (Down's syndrome). Arch Oral Biol 16:707–722.

Hall BK. 1999. Evolutionary developmental biology. Dordrecht: Kluwer Academic. 491 pp.

Hall BK, Miyake T. 1995. Divide, accumulate, differentiate: cell condensation in skeletal development revisited. Int J Dev Biol 39:881–893.

Hall BK, Miyake T. 2000. All for one and one for all: condensations and the intiation of skeletal development. Bioessays 22:138–147.

Hattori M, Fujiyama A, Taylor TD, Watanabe K, Yada T, Park HS, Toyada A, Ishii K, Torold Y, Choi DK, Soeda E, Ohki M, Takagi T, Sakaki Y, Tsudien B, Blechochmidt K, Polley A, Massel U, Dolubur J, Kumpf K, Labmann R, Potterson D, Raiahweld K, Rump A, Schilhabel M, Schurly A, Zim?m W, Rosenbhal A, Kudoh J, Schsbuya K, Kawasaki K, Asakawa S, Shim?ni A, Sasaki T, Nagamine K, Misuyama S, Anoomagazakis SE, Minoshima S, Shimizu N, Nordslek G, Homischer K, Braur P, Scharfe M, Schen O, Desario A, Reiel? J, Kaner O, Blocker H, Ramser J, Beck A, Klager S, Hennig S, Rie?salmann L, Dagand B, Haaf T, Wchrmeyer S, Berzym K, Gardiner K, Nizedt D, Francis F, Lahrach H, Reinhardr R, Yospo M. 2000. The DNA sequence of human chromosome 21. Nature 405:311–319.

Horowitz S, Shapiro H. 1951. Modification of mandibular architecture following removal of tempoarlis muscle in the rat. J Dent Res 30:276–280.

Kisling E. 1966. Cranial morphology in Down's syndrome: a comparative roentgencephalometric study in adult males. Ph dissertetron, Copenhagen: Munksgaard. 106 pp.

Kontges G, Lumsden A. 1996. Rhombencephalic neural crest segmentation is preserved throughout craniofacial ontogeny. Development 122: 3229–3242.

LeJeune J, Gauthier M, Turpin R. 1959. Etudes des chromosomes somatiques de neuf enfants mongoliens. CR Acad Sci 248:1721–1722.

Lele S, Richtsmeier JT. 1991. Euclidean distance matrix analysis: a coordinate-free approach for comparing biological shapes using landmark data. Am J Phys Anthropol 86:415–427.

Lele S, Richtsmeier JT. 1995. Euclidean distance matrix analysis: confidence intervals for form and growth differences. Am J Phys Anthropol 98:73–86.

Lele S, Richtsmeier JT. 2001. An invariant approach to the statistical analysis of shapes. London: Chapman and Hall/CRC Press.

Moore WJ. 1973. An experimental study of the functional components of growth in the rat mandible. Acta Anat 85:378–385.

Moss ML, Meehan MA. 1970. Functional cranial analysis of the coronoid process in the rat. Acta Anat 77:11–24.

Richtsmeier JT, Lele S. 1993. A coordinate-free approach to the analysis of growth patterns: models and theoretical considerations. Biol Rev Camb Philos Soc 68:381–411.

Richtsmeier JT, Baxter LL, Reeves RH. 2000. Parallels of craniofacial maldevelopment in Down syndrome and Ts65Dn mice. Dev Dyn 217: 137–145.

Sago HC, Carlson E, Smith D, Kilbridge J, Rubin E, Mobley W, Epstein C, Huang T. 1998. Ts1Cje, a partial trisomy 16 mouse model for Down syndrome, exhibits learning and behavioral abnormalities. Proc Natl Acad Sci U S A 95:6256–6261.

Sago H, Smith DJ, Rubin EM, Crnic LS, Huang TT, Epstein CJ. 2000. Genetic dissection of region associated with behavioral abnormalities in mouse models for Down syndrome. Pediatr Res 48:606–613.

Thelander H, Pryor H. 1966. Abnormal patterns of growth and development in mongolism. Clin Pediatrics 5:493–501.

Washburn S. 1947. The effect of the temporal muscle on the form of the mandibles [Abstract]. J Dent Res 26:174.